PAPER

Development of a Sonar System to Estimate the Seafloor Subsurface Burial Depth of a Towed Gamma-Ray Spectrometer

AUTHORS

Yoshihiro Hirao
Seiki Ohnishi
National Maritime Research Institute, Tokyo, Japan

Blair Thornton
Institute of Industrial Science, The University of Tokyo

Yusuke Yano
Hakuyodo Co., Ltd., Kanagawa, Japan

Naoteru Odano
Tamaki Ura
National Maritime Research Institute, Tokyo, Japan

ABSTRACT

A sonar system and image processing method have been developed to continuously estimate the seafloor subsurface burial depth of a gamma-ray spectrometer that is towed along the seafloor by a ship. The towed gamma-ray spectrometer, called the RESQ hose, is an instrument designed to measure radiation levels in seafloor sediments that were contaminated as a result of the accident at the Fukushima-Daiichi nuclear power plant. *In situ* measurements of subsurface burial depth can increase the accuracy of the radionuclide concentration levels estimated by the RESQ hose by allowing for more accurate modeling of the measurement conditions. The reliability of the system is verified through sea trials performed near the outlet of the Abukuma River. Continuous measurements of burial depth are achieved with an outlier ratio of less than 5%. The burial depths measured by the device show a strong correlation with the acoustic backscatter intensity of side-scan sonar images obtained along the surveyed transect, indicating that burial depth is dependent on sediment type. We examine the influence of burial depth on the conversion factors between detected gamma-ray count rates and the concentrations of ^{134}Cs and ^{137}Cs. For both nuclides, the calculated factors increase by nearly 80% as burial depth increases from 0 to 11 cm. The converted results from the measured ^{137}Cs count rates are compared with a core sample obtained near the transect, with the nearest point within a factor of two of the sampling result.

Keywords: Fukushima-Daiichi nuclear power plant, profiling sonar, ship-towed gamma-ray spectrometer, radioactive marine sediments, burial depth

Introduction

The accident at the Fukushima-Daiichi nuclear power plant resulted in a large amount of radioactive material being released into the environment. In order to determine the distribution of radioactive material on the seafloor, a ship-towed gamma-ray spectrometric device, called the RESQ hose, has been developed to continuously map the distribution of ^{134}Cs and ^{137}Cs in marine sediments (Thornton et al., 2013a, 2013b). The RESQ hose consists of a NaI(TI) scintillation spectrometer (Knoll, 2000) built into an 8-m-long rubber hose that is towed along the seafloor by a ship. During operation, the hose is towed along the seafloor at about 2 knots to make continuous *in situ* measurement of gamma rays emitted from radionuclides in the sediments. The device measures the gamma-ray spectrum between 0.1 and 1.8 MeV, and the count rates of each photoelectric peak are used to estimate the concentrations of radionuclides on the seafloor using a radiation transport model of the hose and its surroundings. However, in order to convert the measurements of the device to radioactive concentrations accurately, information concerning the conditions at which measurements were made must be known. The information is mainly composed of three parameters: the burial depth of the RESQ hose into seafloor, the vertical distribution of radionuclides below surface of seafloor, and the sediment type. While information about the sediment type and vertical distribution of radionuclides can be determined from samples obtained in the area, accurate estimation of the burial depth requires continuous *in situ* measurement. The objective of this study is to develop a method to estimate the burial depth of the hose during towed operation and examine its influence on the factors to convert gamma-ray count rates to radioactivity concentration measurements.

FIGURE 1

Overview of the sonar system. (a) PC-battery case. (b) Sonar case. (c) Full view.

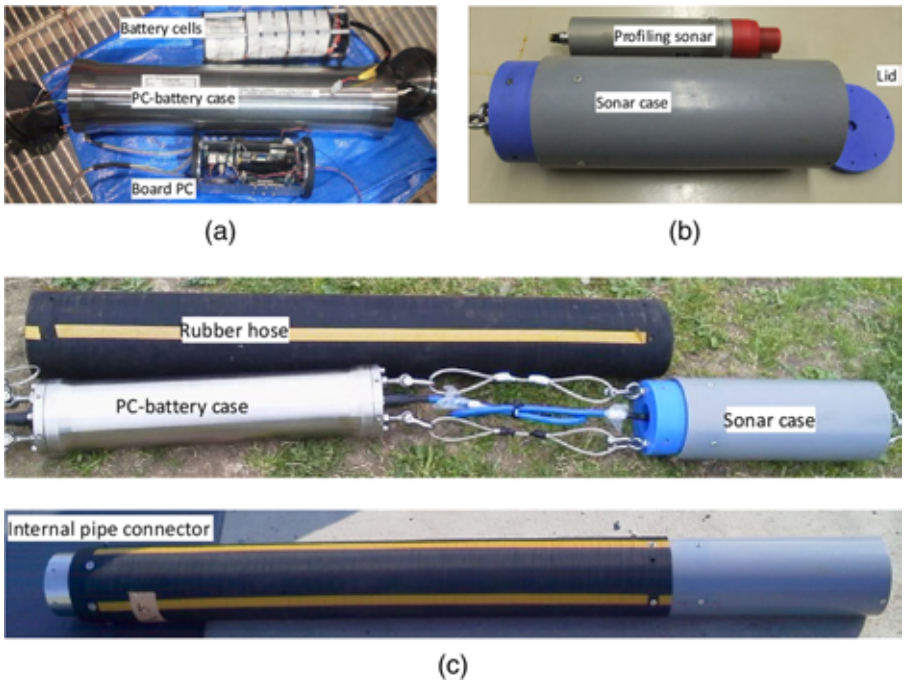

First, we describe a sonar system designed to continuously observe the surface of the seafloor relative to the towed system, together with methods to process the sonar images to estimate burial depth in a quantitative manner. The system consists of a profiling sonar built into a PVC case that can be attached to the RESQ hose. Next, we describe sea trials performed during March 2013 at the Abukuma River mouth, located 80 km north of the Fukushima-Daiichi Nuclear power plant, in order to test the applicability of the proposed system. To examine the relationship between burial depth and sediment type, the results estimated using our system are compared with the acoustic intensity of side-scan sonar images obtained along the surveyed transect. Finally, the conversion factors to quantify the radiation measurement are calculated, and the influence of burial depth on the accuracy of the system is assessed. The measured gamma-ray count rate data are converted to radionuclide concentration using the calculated conversion factors, and the results are compared with a laboratory-analyzed core samples obtained near the surveyed transect for verification.

Sonar System for Observing Burial of the RESQ Hose Into the Seafloor

The sonar system developed for observing the subsurface burial of the hose consists of an IMAGENEX model 831L profiling sonar (Imagenex, 2014), a board PC, and Li-ion battery cells. Figure 1 shows an overview of the system, and Figure 2 shows its schematic. The sonar is stored in a PVC case. Both the PC and battery cells are stored in a water-tight, pressure-resistant stainless case. The two cases are connected using two tension-bearing wire ropes and an underwater cable, through which the sonar communicates with the PC and power is supplied from the battery cells. The PC-battery case is covered with a rubber hose to protect it from mechanical impact and abrasion during towed operation.

FIGURE 2

Schematic of the sonar system.

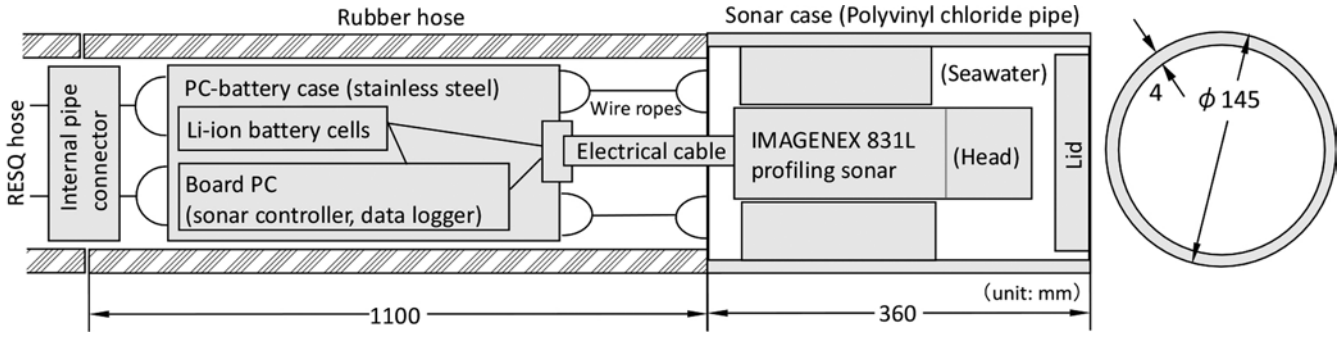

FIGURE 3

Schematic diagram of the sonar system attached to the RESQ hose.

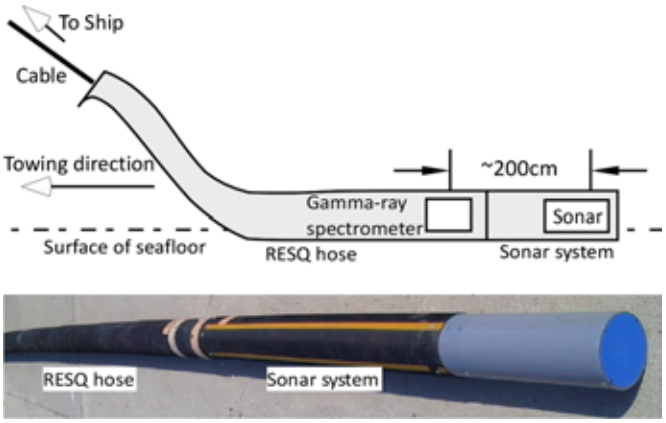

The rubber hose is connected to the sonar case, both of which are cylindrical with the same outer diameter as the RESQ hose to minimize the risk of snagging.

The sonar emits a 2.25-MHz high-frequency acoustic signal from inside the case to continuously scan a 360-degree cross-sectional profile of the surrounding seafloor. The data are logged by the board PC, and the system operates as a standalone device with the battery cells supplying enough energy for more than 8 h of continuous operation. The device is attached to the RESQ hose using two wire ropes that connect the PC-battery case to aft end of the RESQ hose, and the rubber hoses are linked using an internal pipe connector, as shown in Figure 3. During operation, the sonar is located about 2 m aft of the RESQ hose's gamma-ray spectrometer. The separation between the sonar and the spectrometer is relatively short compared to the total length of the system, and for the purpose of this study, the burial depth measured by the sonar is assumed to be the same as that of the spectrometer.

The appropriate sonar settings and material to use for the sonar case were determined by testing various setups in a small water-filled tank. The system was buried at various depths in a soil/sand sediment mixture, and six different casing materials were tested. A hard PVC pipe was found to have better acoustic transparency compared to stainless steel, aluminum, acrylic resin, hard nylon, and polyester pipes that were also tested. A pipe thickness of 4 mm was chosen considering the trade-off between acoustic transparency and durability during towed operation. The sonar gain was set at 29 dB with a range of 50 cm to give a clear image of interface between water and soil, without suffering from excessive ringing. The system specifications are summarized in Table 1.

During operation, small holes in the lid allow the sonar case to fill with water. In order to prevent sediments entering the case and interfering with the signal, it is necessary to wait for a few minutes until the case is filled with clean seawater before it reaches the seafloor. This is achieved through operational protocol when the device is deployed at sea.

TABLE 1

Specification of the sonar system.

General specification	
Length (m)	1.46
(plus RESQ hose) (m)	9.46
Diameter (m)	0.145
Weight in air (kg)	28
Maximum water depth (m)	500
Profiling Pipe Sonar	
Model	IMAGENEX 831L
Dimensions (mm)	φ61 × 343
360-degree scan period	>1.3 s
Built-in	Pitch/roll sensor
Gain (dB)	29
Range in radius (mm)	500
PC and Battery Cells	
Board PC	Intel Atom, 5 V, 2-GB RAM
Communication	Ethernet
Power supply	Li-ion 6P7S, 25 V, 12 Ah

Estimation of Burial Depth From the Sonar Images

The burial depth of the RESQ hose into the seafloor can be estimated by processing acoustic images of the seafloor obtained by the sonar system during operation. Figure 4(a) shows an example of a 360-degree cross-section of the system and the seafloor measured by the sonar during the survey at the Abukuma River mouth, described in the next chapter. Figure 4 (b) shows the same image that has been labeled to show the relevant results of the data processing method. The white circle indicates periphery of the sonar case (PSC). The orange horizontal line indicates the bottom level of the sonar case (BLC). The two white lines indicate the estimated surface of seafloor on the left (SLC) and right (SRC) sides of the case, respectively. The large black region below the surface indicates the volume of seafloor through which the acoustic signal could not penetrate. The red, yellow, green, and blue regions scattered above the surface are thought to be from near-bottom suspended particulate matter. The image shows different levels for the intersection of SLC and SRC with the case. It suggests that the surface is sloping or the burial depth is slightly changing while towing. We define the burial depth (BD, red arrow in the figure) as the average of the distance from LP and RP to BLC, where LP indicates an intersection point between SLC and PSC and RP indicates one between SRC and PSC. In some cases, the surface line in the acoustic image appears jagged as shown in Figure 4(c), and under some conditions, the surface of the seafloor cannot be identified, as shown in Figure 4(d). Possible reasons for such observations are discussed later in the discussion section of this paper.

Figure 5 shows a flowchart of the sonar image processing procedure. The processing pipeline is implemented using OpenCV image processing libraries (OpenCV, 2014). The processing method to extract SRC from the image is as follows. The original image is converted to grayscale and then binarized with the threshold value of 10 on a 0–255 scale. Then, the binary image is dilated three times, eroded seven times, and again dilated twice to eliminate notches, small holes, and clumps in the data and so to keep only continuous regions and surfaces.

FIGURE 4

Examples of sonar images obtained during deployment at the Abukuma River mouth. (a) Original scan image by the profiling sonar. (b) Image with indication symbol of processing methods. (c) Example of jagged surface and failed surface detection. (d) Example of indistinct surface for soft, silty seafloor sediments.

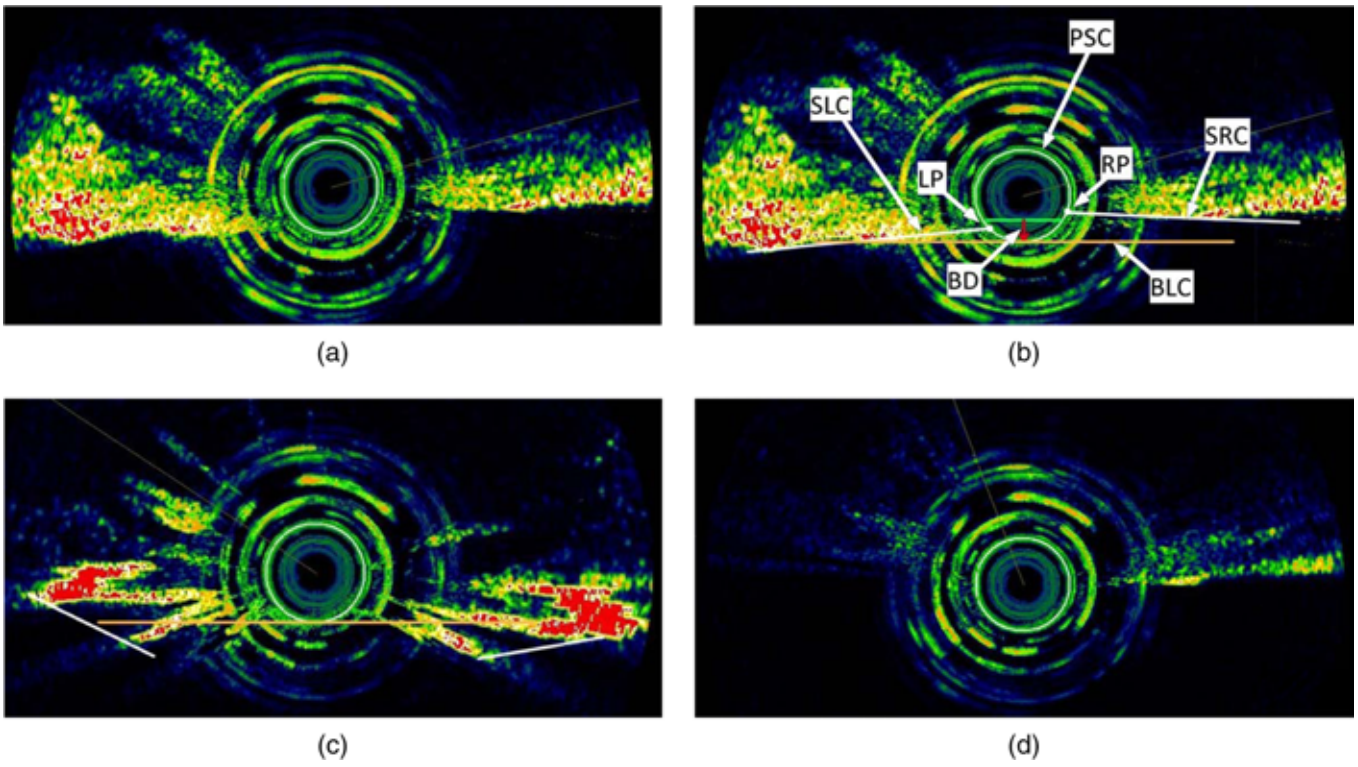

FIGURE 5

Flowchart of image processing to determine burial depth from sonar data.

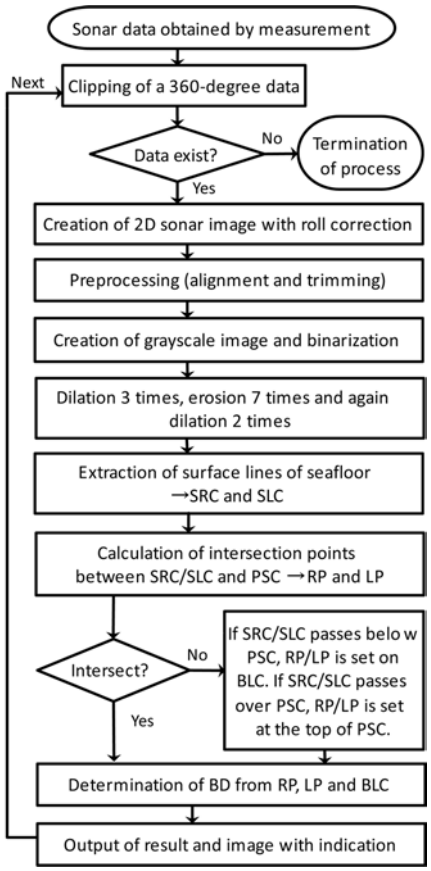

To determine the location of the seafloor, we use 10 points (green points in Figure 6) by scanning the pixel values upward from the bottom of the sonar image along 10 vertical lines (yellow lines) until a reflection signal is detected, that is, the line intersects a white pixel. Then, SRC/SLC can be extracted as the probable surface line of seafloor (red line) by determining the line of best fit through the points. When the interpolated line does not intersect PSC, RP/LP are determined based on a positional relation between SRC/SLC and PSC. If SRC/SLC passes below PSC, as seen in Figure 4(c), RP/LP is set on BLC. If SRC/SLC passes over PSC, RP/LP is set at the top of PSC. This is a temporary solution for missing the intersection point due to surface slope error of SRC/SLC. Finally, the estimated results are verified by visual inspection of the labeled output images. Through the survey, it was found that a surface line cannot be detected as expected for a jagged surface and indistinct surfaces as shown in Figures 4(c) and 4(d). In such cases, the result is rejected and replaced by an interpolated value between the preceding and next reliable data.

FIGURE 6

Extraction of surface line of seafloor from binarized image.

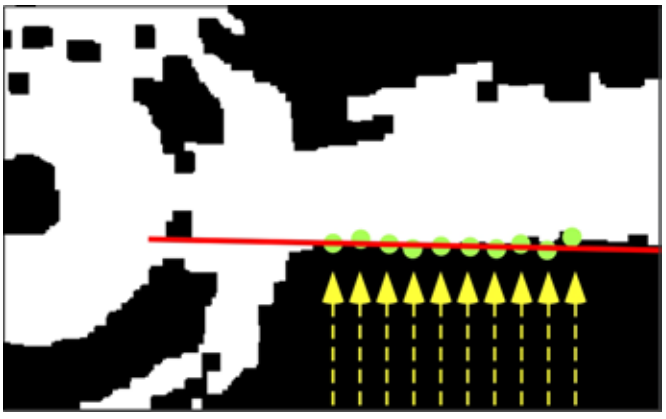

Measurement Results

The sonar system attached to the RESQ hose was tested for a linear transect of 3.5 km during a monitoring survey at the Abukuma River mouth off Miyagi on March 13, 2013. The device was towed by a 10-tonne fishing vessel at a speed of 2 knots. Prior to the survey, an acoustic survey of the seafloor was performed using a shipboard side-scan sonar along the same transect to determine the sediment type along the transect. Figure 7 shows the side-scan sonar image along the east-west transect. Core sampling of sediments was carried out at two stations, St.1 and St.2, on March 15. Regarding the towed operation, the boat starts about 100 m east of St.2 and crosses near St.1, and the transect ends at the east of the transect. In the acoustic images, the image becomes darker as the intensity of reflection becomes weaker, that is, the surface sediments become softer. Based on qualitative comparison with sediment core samples obtained in the survey area, it is considered that the lighter part represents coarse sand or rocky outcrop, and the darker part represents silt or clay.

Figure 8 shows the burial depth of the hose estimated from sonar images continuously obtained by the system described in this work. As a result of visual inspection, the ratio of outliers compared to the total number of scan images was less than 5%. The reflection intensity of data obtained by the side-scan sonar is also shown for comparison. The intensity data are in arbitrary units where 1 corresponds to the hardest sediments and 255 is the softest sediments measured during this survey. It is shown that the momentary burial depth of the device can vary widely up to 14 cm, where the device is almost fully buried. However, this only accounts for a small part of the survey data, and for 84% of the measurements, the hose depth remains

FIGURE 7

Ship-towed transect and core sampling stations in monitoring survey at the Abukuma River mouth.

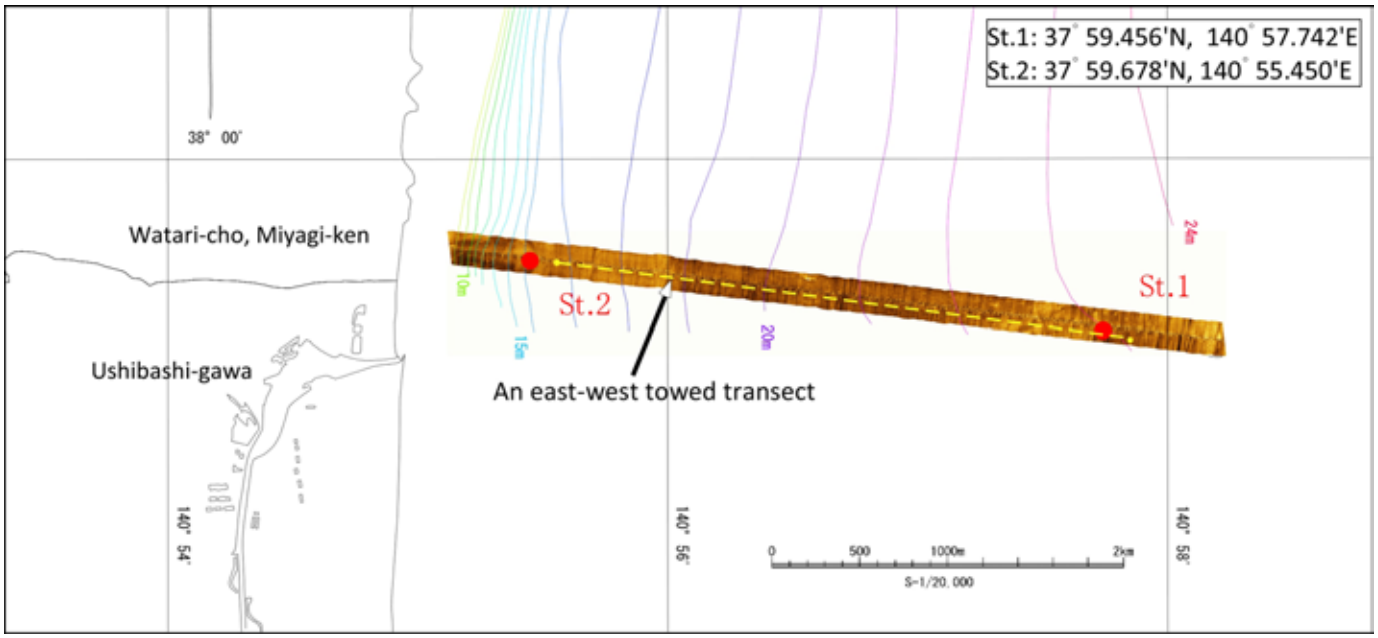

between 0 and 5 cm. The mean value and standard deviation of the hose depth through the survey are 2.2 and 2.4 cm, respectively. The depth of burial between 09:13 and 09:24 and between 09:51 and 09:58 is between 0 and 5 cm. This is also supported by the fact that the side-scan values are small (i.e., strong reflections) at the corresponding positions, suggesting that the bottom is hard and consists of coarse sand sediments. In contrast, the burial depth is mostly larger than 5 cm at around 09:25 and between 09:36 and 09:46. The larger values for the side-scan data indicate weak reflections, suggesting that the bottom is soft and consists of silty clay sediments. Figure 9 shows moving average trendlines of both the burial depth and acoustic intensity with 60 points for each type of data measured along the transect. The positions of peaks and valleys show a strong correspondence to the acoustic reflection intensity, indicating that there is a correlation between the burial depth of the device and the sediment type.

FIGURE 8

Distribution of burial depth estimated by the sonar system along the transect and seafloor-echo data obtained by onboard side-scan sonar.

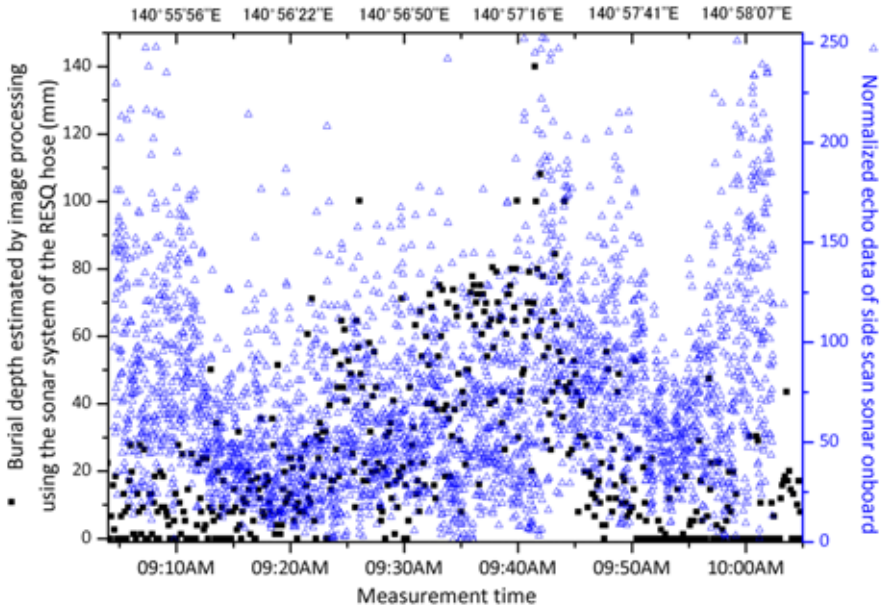

Influence of Burial Depth of the RESQ Hose on the Radioactivity Conversion Factors

The influence of burial depth of the hose on the radioactivity conversion factors has been examined. The

FIGURE 9

Moving average trendlines of the burial depth distribution and the seafloor-echo data with 60 points over the transect.

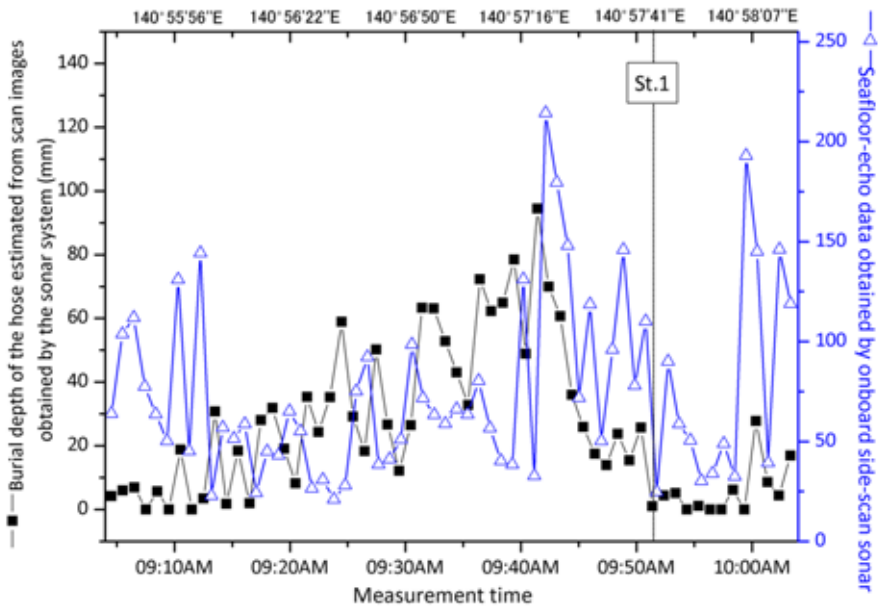

gamma-ray count rates measured by the RESQ hose are converted to radioactive concentrations of the seafloor through Monte Carlo simulation of radiation transport taking into consideration the 3-D geometry of the device and its environment (Thornton et al., 2013a). The Monte Carlo method is widely used to calculate a solution to radiation transport problems (Lewis & Miller, 1993). Other than the burial depth of the hose, the calculated solution depends on the vertical distribution of radionuclides in the sediments and the physical properties of sediments assumed in the simulation. Figure 10 shows two vertical distributions of concentrations for ^{134}Cs and ^{137}Cs that were used to determine the influence on the calculated conversion factors. The first vertical distribution is that measured for the core sample obtained at St.1, shown in Figure 7, where the sediment type was coarse sand. The other is the vertical distribution of the core sample obtained at St.2, where the sediment type was silty clay. The subsurface depth of the core samples are 0–14 cm at St.1 and 0–20 cm at St.2. The depth intervals between which the samples were analyzed are 0–1, 1–2, 2–4, 4–6, 6–10, and 10–14 cm from the surface at St.1, with an additional layer from 14 to 20 cm at St.2. The concentrations deeper than the sampled depth range are assumed to be zero because their distribution profile is unknown. It is also assumed that sediment layers below the hose are not crushed and the vertical distributions are preserved as shown in Figure 11. Table 2 shows properties of different sediment types of the seafloor (Hamilton, 1971; Thornton et al., 2013b). For comparison, coarse sand and silty clay are chosen to be representative of the hard and soft sediments along the survey transect, respectively. Any contributions from radioactive nuclides suspended in seawater are assumed negligible, since the concentration of each radionuclide determined from monitoring surveys off Miyagi during the same period were not more than 0.01 Bq/L in the lower layer of seawater (Nuclear Regulation Authority, 2013). The geometry and materials used for the gamma-ray spectrometer and its environment are the same as those used in the past measurements off Fukushima, described in Thornton et al. (2013a).

Figure 12 shows how much the calculated conversion factors for ^{134}Cs and ^{137}Cs vary with the burial depth of the hose under the assumed conditions. The results of conversion are based on average dry-weight concentrations from 0 to 3 cm below the surface of seafloor. The factors for wet-weight can be calculated by dividing the dry-weight factors by $(1 - u)$, where u is water content of sediment as given in Table 2. The conversion factors for ^{134}Cs are slightly larger than those for ^{137}Cs, where the main photoelectric peak energies of ^{134}Cs and ^{137}Cs are 796 and 662 keV, respectively. Since the gamma-ray energies differ by only 134 keV, their penetration capabilities are similar. For both nuclides, the factors increase gradually by about 80% as the burial depth increases from 0 to 11 cm. However, for the burial depth between 0 and 5 cm mostly shown in the measurement, the difference in the conversion factors is about 45%. The negative depth indicates the distance between the bottom of the hose and the surface of seafloor when the hose is not in contact with the seafloor. This situation may occur when the hose bounces on hard and bumpy surfaces. When the hose lifts off the seafloor by 2 cm, the conversion factors decrease by only 25% compared to when the hose is resting on the

FIGURE 10

Vertical distributions of radioactivity concentrations of ^{134}Cs and ^{137}Cs below surface of seafloor based on core sampling.

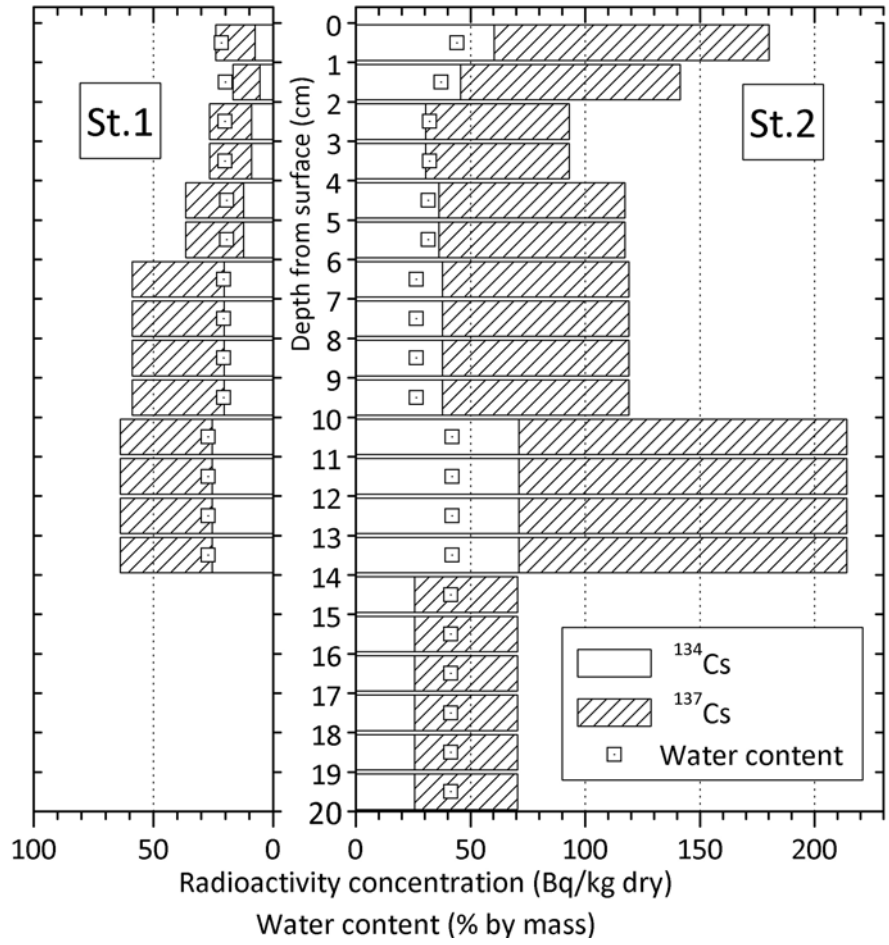

sediment surface, that is, at 0 cm. The change in the conversion factor when the hose loses contact with the seafloor by just a few centimeters is small due to contributions from the surface of the surrounding seafloor.

FIGURE 11

Sediment layer model below the RESQ hose assumed in the conversion factor calculation.

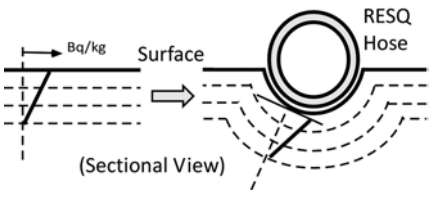

The conversion factor curves are however different for the different nuclide vertical distribution profiles. For ^{137}Cs at the same burial depth, the factors for the distributions of St.1 are around 40% and 50% larger than the factors for St.2 for coarse sand and silty clay sediments, respectively. Regarding the influence of sediment type, the factors for wet-weight do not depend much on the properties of the sediments and are within ±5% for the coarse sand silty clays for the same vertical distributions at each burial depth condition. This is because the value of the mass attenuation coefficient does not depend much on material.

For practical use, the conversion factor curves are fitted by linear regression. The parameters and ranges of the fitting functions are summarized in Table 3. The conversion factors for other sediment types shown in Table 2 lie between the curves of coarse sand and of silty clay. Using the appropriate conversion factors, the measured peak counts of ^{137}Cs are converted to nuclide concentrations along the transect shown in Figure 7. It is assumed that the sediment type is coarse sand with vertical distributions of St.1 if the

TABLE 2

Properties of sediment types of seafloor (Thornton et al., 2013b).

Sediment Type	ρ_{bulk} (g/cm^3)	Water Content, u (% by mass)
Coarse sand	2.03	19.5
Find sand	1.98	22.7
Very find sand	1.91	25.4
Silty sand	1.83	29.6
Sandy silt	1.56	44.8
Sandy silt-clay	1.58	43.7
Clayey silt	1.43	53.8
Silty clay	1.42	54.9

FIGURE 12

Conversion factors of ^{134}Cs and ^{137}Cs calculated for different burial depths of the RESQ hose. (a) ^{134}Cs. (b) ^{137}Cs.

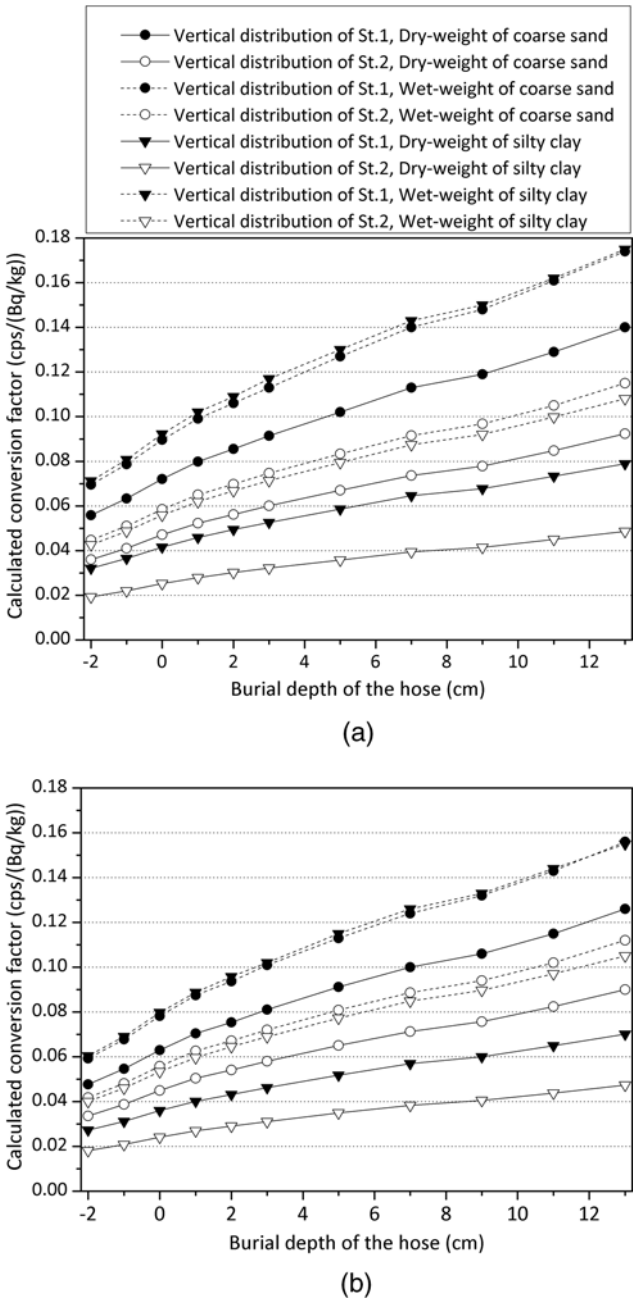

burial depth is less than 5 cm and is silty clay with the distributions of St.2 otherwise. Figure 13 shows a part of the results near the core sampling result of St.1. A trend of rapidly reducing concentrations can be seen in the towed measurement towards the west even over a short distance of a few hundred meters. This indicates that types of the bottom sediment change sharply in this area, as shown in Figure 9, and therefore, the results of sampling may also vary greatly (Kusakabe et al., 2013). Nevertheless, the absolute value of the nearest point on the transect from St.1 is within a factor of two of the sampling result. This demonstrates that the calculated factors can be applied with good accuracy. The cause of error could be related to the misalignment of sampling position relative to the transect and the difference in vertical distribution.

Discussion

The resolution of the sonar images obtained by our system is sufficient to estimate the burial depth of the RESQ hose. However, it is still difficult to detect a surface line from images that have jagged or indistinct surfaces as shown in Figures 4(c) or 4(d), respectively. A possible cause for the jagged surfaces in some of the measurements is physical motion of the system during the time taken to complete a 360-degree scan profile. A lap of scan takes about 5 s due to the time taken to log the data. For this reason, effects of rapid roll and pitch motion of the sonar may cause artifacts in the measurements. Introducing a faster processor to log the data is expected to significantly reduce these effects by shortening the scan period. The indistinct surfaces mostly appear on soft seafloor, where the system is more deeply buried. In our future work, we will investigate the use of variable gain control to optimize the quality of the image for the observed depth of burial conditions, and it may be possible to distinguish the surface under these conditions by actively increasing the acoustic gain when the system is more deeply buried.

Through the experiments described, it can be seen that the system may also provide valuable information to understand the sediment type of the seafloor where the RESQ hose is

TABLE 3

Linear fitting parameters for calculated conversion factors.

Nuclide	Vertical Distribution of Concentrations	Sediment Type	Weight	Conversation Factor (cps/[Bq/kg]), $Y = A + BX$		
				Parameter A	Parameter B	Range of Burial Depth, X (cm)
^{134}Cs	St.1	Coarse sand	Dry	0.0718 ± 8.9E–4	0.0064 ± 3.5E–4	$-1 < X < 5$
			Wet	0.0891 ± 1.0E–3	0.0079 ± 4.0E–4	
	St.2	Silty clay	Dry	0.0281 ± 7.4E–4	0.0016 ± 7.9E–5	$5 \leq X$
			Wet	0.0620 ± 1.6E–3	0.0035 ± 1.7E–4	
^{137}Cs	St.1	Coarse sand	Dry	0.0626 ± 8.6E–4	0.0060 ± 3.3E–4	$-1 < X < 5$
			Wet	0.0778 ± 1.1E–3	0.0074 ± 4.3E–4	
	St.2	Silty clay	Dry	0.0273 ± 6.2E–4	0.0015 ± 6.6E–5	$5 \leq X$
			Wet	0.0603 ± 1.4E–3	0.0034 ± 1.4E–4	

towed. However, it must be noted that the quantitative relations between the burial depth and the sediment type depend on other various conditions. For example, if the system is towed at higher speeds, the depth of burial may possibly become smaller, even for the same type of sediment. In the analysis of the influence of burial depth on the conversion factor, it is assumed that the layers of sediment under the RESQ hose remain uncompressed as illustrated in Figure 11, and the total amount of radioactivity in each layer is preserved. The effect of towing a hose on the structure of the surrounding sediment layers has not previously been studied, and it is possible to imagine two other types of model. One is a model where the layers under the hose are compressed by different amounts similar to streamline contours around a cylinder as shown in Figure 14(a). Another possibility is a scrape model where the layers are scraped by the hose as shown in Figure 14(b). In reality, these models may be mixed, and the actual situation may well depend on sediment type. In order to examine the influence of the different model types on the conversion factors used for quantification, the relative values for our uncompressed layer preserved model and the scrape model are compared in Figure 15. It is shown that the

FIGURE 13

Results of concentrations converted from gamma-ray measurements of ^{137}Cs along the transect and a core sampling result.

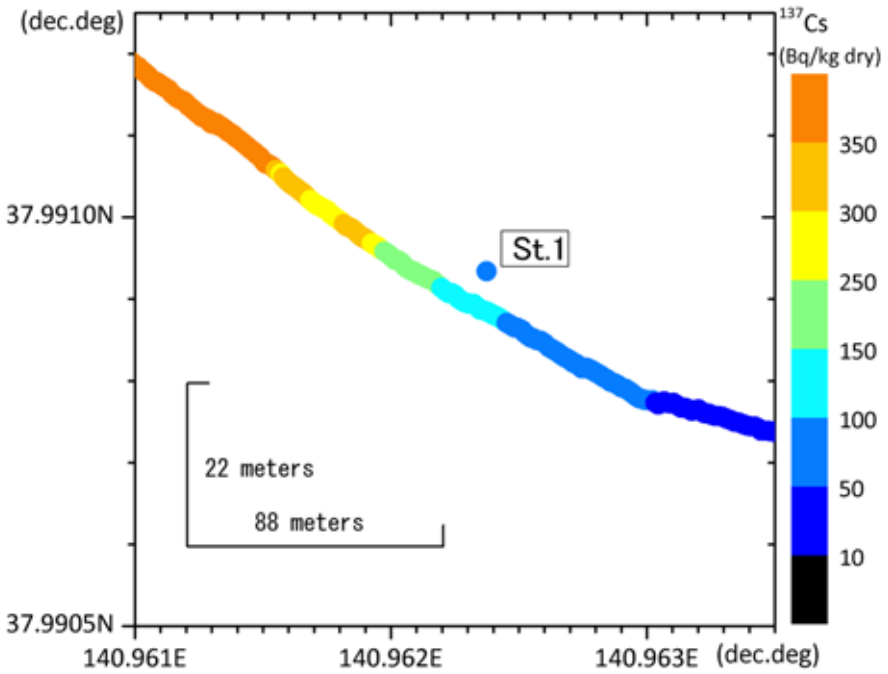

FIGURE 14

Other sediment layer models below the RESQ hose. (a) Streamline. (b) Scrape.

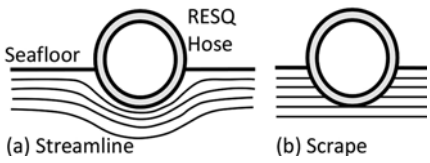

FIGURE 15

Relative values of conversion factors of ^{137}Cs calculated for different layer models.

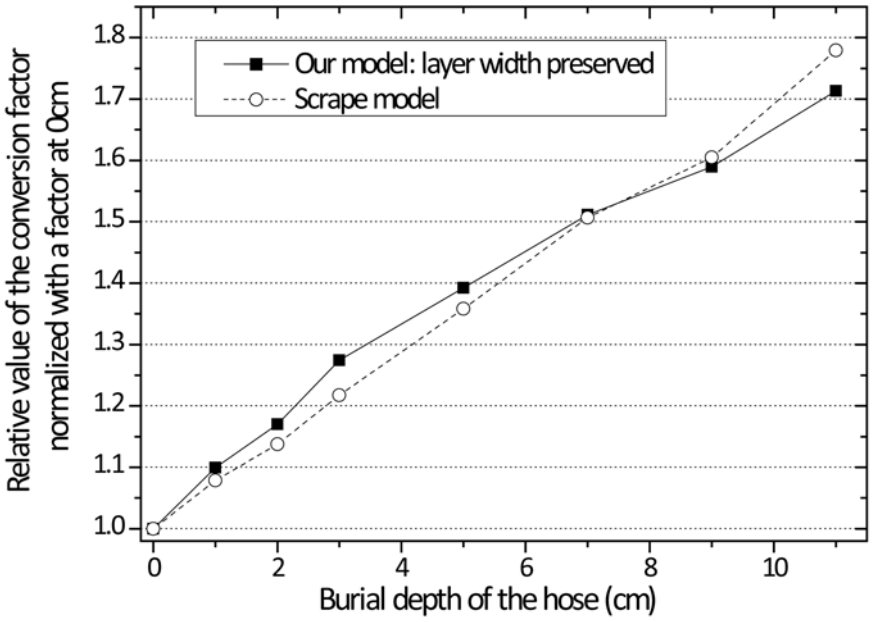

difference between the factors for the two models is <5%, and so, it can be concluded that the sensitivity of the results to the type of model used is relatively small.

Conclusions

We have given an overview of a sonar system and methods to estimate the burial depth of the RESQ hose into seafloor sediments during towed radiation monitoring surveys. The reliability of the system was verified at sea during a monitoring survey along a transect near the Abukuma River mouth. The ratio of burial depth detection outliers to the total number of profile measurements is <5%. When the depth distribution is compared with the acoustic intensity of shipboard side-scan sonar measurements, a strong correlation is found indicating that the depth of burial of the hose is dependent on the seafloor sediment type. The results demonstrate that the developed system is sufficiently reliable for practical use and further show that the measured results are also useful to predict the sediment type. Based on our examination of the influence of burial depth on the conversion factors between the photoelectric peak counts and the concentrations of ^{134}Cs and ^{137}Cs, it is found that the calculated conversion factors increase by 80% as the depth increases from 0 to 11 cm. However, for 84% of the measurements, the depth of burial remains between 0 and 5 cm, for which the difference in the conversion factors is about 45%. The influence of the vertical distribution of radionuclides is shown to have a strong influence on the conversion factors, where for the two different distributions assumed in this work, the difference was as much as 50%. With regard to different types of sediments, once converted to wet-weight measurements, the influence of sediment type is small. The method proposed in this work has important implications for future radiation monitoring surveys using towed gamma-ray spectrometers and can increase the accuracy of measurements by accounting for the depth of burial of the instrument during each measurement. The converted results for ^{137}Cs measurements along the transect are compared with core samples obtained in the area. The measured concentration of the nearest point from the sample is within a factor of 2, where the difference in the measured levels can be well explained by a sharp change in sediment type near the region where the sample was obtained. It is hoped that the system proposed in this work can help determine the distribution of radioactive material on the seafloor after the Fukushima-Daiichi nuclear power plant and help form a basis to plan recovery strategies.

Acknowledgments

The authors are grateful to Dr. Shuhei Fujimoto of National Maritime Research Institute; Mr. Naoki Katsuta of Kowa Co., Ltd.; and Mr. Daigo Kirimura of Azumino Electric Components for their support during development. This research was funded by the Fishery Agency of Japan.

Corresponding Author:

Yoshihiro Hirao
National Maritime Research Institute
6-38-1 Shinkawa, Mitaka-shi,
Tokyo 181-0004, Japan
Email: tora@nmri.go.jp

References

Hamilton, E.L. 1971. Elastic properties of marine sediments. J Geophys Res. 76:579-604. http://dx.doi.org/10.1029/JB076i002p00579.

Imagenex Technology Corp. 2014. IMAGENEX model 831L digital pipe profiling sonar. Available at: http://www.imagenex.com/html/831l.html (accessed 01 April 2014).

Knoll, G.F. 2000. Radiation Detection and Measurement (3rd Edition), p. 326. Hoboken, NJ: John Wiley & Sons, Inc.

Kusakabe, M., Oikawa, S., Takata, H., & Misonoo, J. 2013. Spatiotemporal distributions of Fukushima-derived radionuclides in surface sediments in the waters off Miyagi, Fukushima, and Ibaraki Prefectures, Japan. Biogeosci Discuss. 10:4819-50. http://dx.doi.org/10.5194/bgd-10-4819-2013.

Lewis, E.E., & Miller, W.E., Jr. 1993. Computational methods of neutron transport. Am Nucl Soc.

Nuclear Regulation Authority. 2013. Distribution map of radioactivity concentration in the seawater around coast of Miyagi Prefecture (Based on the press release of TEPCO) Sampling Date: Mar 5, 2013. Available at: http://radioactivity.nsr.go.jp/ja/contents/8000/7389/24/229_2_0419.pdf (accessed 01 April 2014).

OpenCV. 2014. Open source computer vision library. http://opencv.org/ (accessed 01 April 2014).

Thornton, B., Ohnishi, S., Ura, T., Odano, N., & Fujita, T. 2013. Continuous measurement of radionuclide distribution off Fukushima using a towed sea-bed gamma ray spectrometer. Deep-Sea Res. Pt. 1(79):10-19. http://dx.doi.org/10.1016/j.dsr.2013.05.001.

Thornton, B., Ohnishi, S., Ura, T., Odano, N., Sasaki, S., Fujita, T., … Ambe, D. 2013. Distribution of local ^{137}Cs anomalies on the seafloor near the Fukushima Dai-ichi Nuclear Power Plant. Mar Pollut Bull. 74(1):344-350. http://dx.doi.org/10.1016/j.marpolbul.2013.06.031.